

# Causal Discovery on Higher-Order Interactions

**Alessio Zanga\***

A.ZANGA3@CAMPUS.UNIMIB.IT

*Models and Algorithms for Data and Text Mining Laboratory (MADLab),  
Department of Informatics, Systems and Communication (DISCo),  
University of Milano - Bicocca, Milan, Italy*

**Marco Scutari**

SCUTARI@BNLEARN.COM

*Istituto Dalle Molle di Studi sull’Intelligenza Artificiale (IDSIA),  
Lugano, Switzerland*

**Fabio Stella**

FABIO.STELLA@UNIMIB.IT

*Models and Algorithms for Data and Text Mining Laboratory (MADLab),  
Department of Informatics, Systems and Communication (DISCo),  
University of Milano - Bicocca, Milan, Italy*

**Editors:** will be added by editors

## Abstract

Causal discovery combines data with knowledge provided by experts to learn the DAG representing the causal relationships between a given set of variables. When data are scarce, bagging is used to measure our confidence in an average DAG obtained by aggregating bootstrapped DAGs. However, the aggregation step has received little attention from the specialized literature: the average DAG is constructed using only the confidence in the individual edges of the bootstrapped DAGs, thus disregarding complex higher-order edge structures. In this paper, we introduce a novel theoretical framework based on higher-order structures and describe a new DAG aggregation algorithm. We perform a simulation study, discussing the advantages and limitations of the proposed approach. Our proposal is both computationally efficient and effective, outperforming state-of-the-art solutions, especially in low sample size regime and under high dimensionality settings.

**Keywords:** Causal discovery; model averaging; higher-order structures.

## 1. Introduction

Causal graphs are one of the main drivers of modern causal inference (Pearl et al., 2016; Hernán and Robins, 2020). A causal graph is a directed acyclic graph (DAG) used to describe the cause-effect relationships between a given set of variables. A causal graph can be provided by domain experts, learnt from available data, typically observational, or obtained by combining domain experts’ knowledge with the available data.

Causal discovery is the problem of recovering the causal graph by relying solely on the available data or combining data with domain expert knowledge (Glymour et al., 2019; Zanga et al., 2022b). In the last decade, causal discovery has been applied to several scientific fields, including biology (Sachs et al., 2005; Acerbi et al., 2014, 2016), psychology (Miley et al., 2021), medicine (Imoto et al., 2002; Zanga et al., 2022a, 2023) and others (Runge et al.,

---

\* Corresponding author.

2019; Hünermund and Bareinboim, 2019; Addo et al., 2021). While the literature has investigated how to learn a DAG from observational data (Spirtes et al., 2000; Spirtes and Zhang, 2016; Huang et al., 2018), interventional data (Triantafillou and Tsamardinos, 2015; Kocaoglu et al., 2019) and incorporating prior knowledge (Constantinou et al., 2023), the causal discovery problem is far from being solved. This is especially the case for real-world applications where data have a small sample size (Malinsky and Danks, 2018), missing values (Scutari, 2020; Tu et al., 2018; Liu and Constantinou, 2022) or hidden variables (Bongers et al., 2021). In these settings, it is of paramount importance to provide an estimation of the uncertainty of the recovered causal graph. Approaches such as bagging provide a measure of *confidence* (Friedman and Koller, 2003; Eaton and Murphy, 2007) in the inclusion of individual edges into an *average DAG* obtained from a set of candidate DAGs. This is an effective yet coarse summary of the complex cause-effect relationships between variables due to its local nature: each edge involves only two variables. To better mitigate the biases present in real-world observations and preserve more complex patterns of causal relationships, *we focus instead on higher-order structures that involve multiple variables*.

The main contributions of this paper are:

- the definition of *higher-order structures*, that is, structures involving multiple variables, to represent complex edge patterns;
- the design of a novel model averaging algorithm where the aggregation step leverages the concept of higher-order structure;
- a simulation study showing the advantages and limitations of the proposed approach, especially in the small sample size regime and under high dimensionality settings.

The rest of the paper is organized as follows. Section 2 provides the necessary background. Section 3 introduces our framework for model averaging on higher-order structures and the corresponding aggregation algorithms, which are evaluated in Section 4 in a large simulation study. Finally, Section 5 presents our conclusions and future research directions.

## 2. Preliminaries

*Bayesian networks* (BNs; Koller and Friedman, 2009) are a foundational model to encode the interactions between random variables.

**Definition 1 (Bayesian Network)** *Let  $\mathcal{G}$  be a DAG, let  $\mathbf{X}$  be a vector of random variables and let  $P(\mathbf{X})$  be a probability distribution with parameters  $\Theta$ . A Bayesian network  $\mathcal{B} = (\mathcal{G}, \Theta)$  is a probabilistic graphical model where each variable in  $\mathbf{X}$  is associated with a vertex of  $\mathcal{G}$  and the global distribution  $P(\mathbf{X})$  factorizes into local probability distributions according to  $\mathcal{G}$ :*

$$P(\mathbf{X}) = \prod_{X \in \mathbf{X}} P(X | \Pi_X),$$

*with  $\Pi_X$  the parents set of  $X$ , the set of vertices with an edge into  $X$ .*

Since  $\mathcal{G}$  is a DAG, each edge between two vertices  $(X, Y)$  is a directed edge denoted as  $X \rightarrow Y$ , or  $e_{XY}$  for short. While BNs are probabilistic models, we redefine them as causal models as follows.

**Definition 2 (Causal Edge)** *Let  $\mathcal{G}$  be a DAG, and let  $\mathbf{X}$  be a vector of random variables. The value assigned to each variable  $X \in \mathbf{X}$  is completely determined by the function  $f_X$  given its parents  $\Pi_X$ :*

$$X := f_X(\Pi_X) \quad \forall X \in \mathbf{X}.$$

This definition allows us to interpret the edges of  $\mathcal{G}$  in a non-ambiguous way: it enforces a recursive relationship over the structure of  $\mathcal{G}$ , establishing a chain of functional dependencies. If  $\mathcal{G}$  satisfies Definition 2 then it is called *causal graph* (Pearl, 1995).

**Definition 3 (Causal Network)** *A causal network is a BN where  $\mathcal{G}$  is a causal graph.*

Following Scutari (2013), given a BN model  $\mathcal{B} = (\mathcal{G}, \Theta)$ , its posterior distribution given the data  $P(\mathcal{G}, \Theta | \mathcal{D})$  decomposes into the product of  $P(\mathcal{G} | \mathcal{D})$ , the probability distribution of the graph  $\mathcal{G}$  given the data  $\mathcal{D}$ , and  $P(\Theta | \mathcal{G}, \mathcal{D})$ , the probability distribution of the parameters  $\Theta$  given the graph  $\mathcal{G}$  and the data  $\mathcal{D}$ . Therefore, the problem of learning a BN model  $\mathcal{B}$  from the available data  $\mathcal{D}$  decomposes as follows:

$$\underbrace{P(\mathcal{G}, \Theta | \mathcal{D})}_{\text{Learning}} = \underbrace{P(\mathcal{G} | \mathcal{D})}_{\text{Structure Learning}} \cdot \underbrace{P(\Theta | \mathcal{G}, \mathcal{D})}_{\text{Parameter Learning}}.$$

Following Heckerman et al. (1995), we can write structure learning as:

$$\underbrace{P(\mathcal{G} | \mathcal{D})}_{\text{Posterior Distribution}} \propto \underbrace{P(\mathcal{G})}_{\text{Prior Distribution}} \cdot \underbrace{P(\mathcal{D} | \mathcal{G})}_{\text{Likelihood}}.$$

The causal discovery problem (Zanga et al., 2022a,b; Vowels et al., 2021) consists in recovering the true DAG  $\mathcal{G}^*$  by combining the available data  $\mathcal{D}$  together with domain expert knowledge  $\mathcal{K}$ . In this paper we tackle the causal discovery problem with a *score-based approach*<sup>1</sup>, in which a learning algorithm traverses the *search space*  $\mathbb{G}$  of DAGs while looking for the DAG  $\mathcal{G}^*$  maximizing the posterior  $P(\mathcal{G} | \mathcal{D})$ . In the case of a uniform prior distribution  $P(\mathcal{G})$ , the learning algorithm solves the following optimization problem:

$$\mathcal{G}^* = \arg \max_{\mathcal{G} \in \mathbb{G}} P(\mathcal{G} | \mathcal{D}) \quad \text{with} \quad P(\mathcal{G}) = \frac{1}{|\mathbb{G}|}. \quad (1)$$

An example of such an algorithm is the *Hill-Climbing* (HC; Chickering, 2003) algorithm which starts from an empty DAG  $\mathcal{G}_0$  and evaluates iteratively the addition, deletion or reversal of a candidate edge  $e_{XY}$  w.r.t. a *score function*  $\mathcal{S}$ , often referred to as the *scoring criterion*. At iteration  $i$ , the score of the current candidate DAG  $\mathcal{G}_i$  is compared to that of a new candidate DAG  $\mathcal{G}_{i+1}$ . If the score  $\mathcal{S}_{i+1}$  of  $\mathcal{G}_{i+1}$  is better than the score  $\mathcal{S}_i$  of  $\mathcal{G}_i$ , then the graph  $\mathcal{G}_{i+1}$  becomes the new candidate graph, otherwise  $\mathcal{G}_i$  is retained as the best graph at iteration  $i + 1$ . This iterative process continues until the score of the current best DAG cannot be increased further.

---

1. Refer to Nandy et al. (2018) for a more comprehensive overview of score-based structural learning.

## 2.1. Causal Discovery via Bagging

The search space  $\mathbb{G}$  of DAGs grows super-exponentially (Harary and Palmer, 1973): exhaustive search is unfeasible beyond 20–25 variables (Koivisto and Sood, 2004; Rantanen et al., 2020). Bagging (short for *bootstrap aggregation*) provides a widely-used alternative to full Bayesian model averaging that scales to larger numbers of variables (Friedman et al., 1999; Friedman and Koller, 2003). In essence, it is a two-step algorithm in which we:

1. Bootstrap a set of DAGs  $\mathcal{G}$  learnt from a data set  $\mathcal{D}$  and prior knowledge  $\mathcal{K}$ .
2. Aggregate the bootstrapped DAGs  $\mathcal{G}$  to obtain an *average* DAG  $\hat{\mathcal{G}}$ .

In the first step, we use non-parametric bootstrap (Algorithm 1) to generate a collection of  $n$  data sets  $\mathcal{D}_i$ , with  $i = 1, \dots, n$ , and to learn the associated DAGs  $\mathcal{G}_i$  while exploiting the prior knowledge  $\mathcal{K}$ . The DAGs  $\mathcal{G}_i$  form  $\mathcal{G}$  and can be learnt using any causal discovery algorithm. In the second step, we use  $\mathcal{G}$  to estimate the posterior expectation  $\mathbb{E}[\mathcal{G} \mid \mathcal{D}]$ . We don't include  $\mathcal{K}$  in the posterior expectation for brevity. There are several examples of this type of approach in the literature. Singh (1997) combined the bootstrap step with the Expectation-Maximization algorithm (Lauritzen, 1995) to learn BNs from incomplete data. Friedman et al. (1999) discussed a similar approach and explored the difference between non-parametric and parametric bootstrap. More recently, Rohekar et al. (2018) proposed a new recursive non-parametric bootstrap scheme, while Sugahara et al. (2022) investigated the efficacy of sub-bagging from small samples.

---

### Algorithm 1: Non-Parametric Bootstrap.

---

**Input:** A data set  $\mathcal{D}$ , the prior knowledge  $\mathcal{K}$  and the bootstrap iterations  $n$ .

**Output:** The set of bootstrapped DAGs  $\mathcal{G}$ .

```

1 Function NonParametricBootstrap( $\mathcal{D}, \mathcal{K}, n$ )
2   Initialize the bootstrapped DAG set  $\mathcal{G}$  to the empty set.
3   for  $i = 1, 2, \dots, n$  do
4     Sample  $|\mathcal{D}|$  observations with replacement from  $\mathcal{D}$  to obtain  $\mathcal{D}_i$ .
5     Learn a DAG  $\mathcal{G}_i = \arg \max_{\mathcal{G} \in \mathbb{G}} P(\mathcal{G} \mid \mathcal{D}_i)$  given  $\mathcal{D}_i$  and  $\mathcal{K}$ .
6     Insert  $\mathcal{G}_i$  into  $\mathcal{G}$ .
7   return  $\mathcal{G}$ 

```

---

## 2.2. The Impact of the Acyclicity Constraint

As discussed in Scutari (2013), the acyclicity constraint induces a correlation between the edges present in any DAG learnt from data. This holds for the uninformative uniform prior  $P(\mathcal{G}) \propto 1$  and for any posterior  $P(\mathcal{G} \mid \mathcal{D})$ , where the probabilistic dependencies between the variables further increase the correlation between edges that are part of causal pathways. These correlations are reflected in the posterior expectation  $\mathbb{E}[\mathcal{G} \mid \mathcal{D}]$  in general. If cycles were allowed, the edges of  $\mathcal{G}$ , denoted as  $\mathbf{E}_{\mathcal{G}}$ , would be independent of each other when the prior is uniform. In particular, if we shift the focus from the posterior  $P(\mathcal{G} \mid \mathcal{D})$  of the graph  $\mathcal{G}$  as a whole to the posterior  $P(\mathbf{E}_{\mathcal{G}} \mid \mathcal{D})$  of its edge set  $\mathbf{E}_{\mathcal{G}}$ , we observe:

$$P(\mathcal{G} \mid \mathcal{D}) = P(\mathbf{E}_{\mathcal{G}} \mid \mathcal{D}) = \prod_{\mathbf{e}_{XY} \in \mathbf{E}_{\mathcal{G}}} P(\mathbf{e}_{XY} \mid \mathbf{E}_{\mathcal{G}} \setminus \{\mathbf{e}_{XY}\}, \mathcal{D}) = \prod_{\mathbf{e}_{XY} \in \mathbf{E}_{\mathcal{G}}} P(\mathbf{e}_{XY} \mid \mathcal{D})$$

However, since  $\mathcal{G}$  is a DAG, the posterior of each edge  $P(\mathbf{e}_{XY} | \mathcal{D})$  is different from the posterior of each edge *given the others*  $P(\mathbf{e}_{XY} | \mathbf{E}_{\mathcal{G}} \setminus \{\mathbf{e}_{XY}\}, \mathcal{D})$  in general. Moreover, including  $\mathbf{E}_{\mathcal{G}} \setminus \{\mathbf{e}_{XY}\}$  in the probability term makes the estimation of the marginal probability of each edge  $\mathbf{e}_{XY}$  dependent on the distribution of all other possible edges, which, in turn, is summarized by the expected value  $\mathbb{E}[\mathcal{G} | \mathcal{D}]$ . Intuitively, we would prefer to approximate  $P(\mathbf{e}_{XY} | \mathcal{D})$  or  $P(\mathbf{e}_{XY} | \mathbf{E}_{\mathcal{G}}, \mathcal{D})$  using a smaller subset  $\mathbf{E}_{\mathcal{G}}^* \subset \mathbf{E}_{\mathcal{G}}$  which contains the edges relevant for  $\mathbf{e}_{XY}$ . This idea is inspired by [Scutari \(2013\)](#), who proved that edges that are not incident on a common vertex are uncorrelated for DAGs with up to 7 nodes in  $P(\mathcal{G}) \propto 1$ . He also showed by simulation that this relationship holds for larger DAGs. These findings call for an extended evaluation of potential subsets of  $\mathbf{E}_{\mathcal{G}}$  containing edges strongly correlated with  $\mathbf{e}_{XY}$ , which we discuss in the next section.

### 2.3. Threshold-based Model Averaging

The current state-of-the-art averaging algorithm was initially described in [Singh \(1997\)](#) and independently proposed by [Friedman et al. \(1999\)](#); [Imoto et al. \(2002\)](#) with the addition of a threshold. To our knowledge, no substantial modifications have been investigated so far. Henceforth, we refer to this averaging algorithm as the *Threshold-based Model Averaging* (TMA) algorithm. This algorithm estimates the probability  $P(\mathbf{e}_{XY} | \mathcal{D})$  of including each edge  $\mathbf{e}_{XY}$  into the *average DAG*  $\widehat{\mathcal{G}}$  from the set of bootstrapped DAGs  $\mathcal{G}$  and collects them into a matrix  $\mathbf{C}$  called the *confidence matrix*. The aggregation step constructs the DAG  $\widehat{\mathcal{G}}$  with an edge set  $\mathbf{E}_{\widehat{\mathcal{G}}}$  such that it only contains the edges with the highest confidence. As in [Equation \(1\)](#),  $\mathcal{G}$  approximates a sample from the posterior  $P(\widehat{\mathcal{G}} | \mathcal{D})$  and  $\widehat{\mathcal{G}}$  is then an empirical estimate of  $\mathbb{E}[\mathcal{G} | \mathcal{D}]$ . However, directly aggregating all the edges in  $\mathcal{G}$  may result in a cyclic graph. Therefore, we need to solve a constrained optimization problem to find the  $\widehat{\mathcal{G}}$  with the maximal edge confidence set subject to the acyclicity constraint. We start by redefining the constrained optimization problem over the posterior  $P(\mathbf{E}_{\widehat{\mathcal{G}}} | \mathcal{D})$ :

$$\arg \max_{\widehat{\mathcal{G}} \in \mathbb{G}} P(\widehat{\mathcal{G}} | \mathcal{D}) = \arg \max_{\widehat{\mathcal{G}} \in \mathbb{G}} P(\mathbf{E}_{\widehat{\mathcal{G}}} | \mathcal{D}). \quad (2)$$

Indeed, [Equation \(2\)](#) allows us to link the aggregation algorithm over the edge set  $\mathbf{E}_{\widehat{\mathcal{G}}}$  and the posterior maximization over the search space of DAGs  $\mathbb{G}$ . An approximation of the optimization target  $P(\mathbf{E}_{\widehat{\mathcal{G}}} | \mathcal{D})$  is given by the expected value of the posterior  $\mathbb{E}[\mathbf{E}_{\widehat{\mathcal{G}}} | \mathcal{D}]$ :

$$\arg \max_{\widehat{\mathcal{G}} \in \mathbb{G}} P(\mathbf{E}_{\widehat{\mathcal{G}}} | \mathcal{D}) \approx \arg \max_{\widehat{\mathcal{G}} \in \mathbb{G}} \mathbb{E}[\mathbf{E}_{\widehat{\mathcal{G}}} | \mathcal{D}]. \quad (3)$$

The expectation  $\mathbb{E}[\mathbf{E}_{\widehat{\mathcal{G}}} | \mathcal{D}]$  plays a fundamental role in the aggregation step, providing a point estimate of the posterior  $P(\mathbf{E}_{\widehat{\mathcal{G}}} | \mathcal{D})$  by leveraging the information present in  $\mathcal{G}$ . It is computed as the frequency of inclusion of each edge  $\mathbf{e}_{XY}$  in  $\mathcal{G}$ :

$$\arg \max_{\widehat{\mathcal{G}} \in \mathbb{G}} \mathbb{E}[\mathbf{E}_{\widehat{\mathcal{G}}} | \mathcal{D}] = \arg \max_{\widehat{\mathcal{G}} \in \mathbb{G}} \frac{1}{|\mathcal{G}|} \sum_{\mathcal{G}}^{\mathcal{G}} \sum_{\mathbf{e}_{XY}}^{\mathbf{E}_{\mathcal{G}}} \mathbb{1}_{\widehat{\mathcal{G}}}[\mathbf{e}_{XY} | \mathcal{D}], \quad (4)$$

The outer summation  $\sum_{\mathcal{G}}^{\mathcal{G}}$  aggregates the graphs  $\mathcal{G}$  across the bootstrapped graphs  $\mathcal{G}$ , while the inner summation  $\sum_{\mathbf{e}_{XY}}^{\mathbf{E}_{\mathcal{G}}}$  aggregates the edges  $\mathbf{e}_{XY}$  across the edge sets  $\mathbf{E}_{\mathcal{G}}$ . The indicator

function  $\mathbb{1}_{\widehat{\mathcal{G}}}$  links the average DAG  $\widehat{\mathcal{G}}$  to the objective function of the maximization problem. Wrapping up Equations (2) to (4), the core of TMA is the following optimization problem:

$$\arg \max_{\widehat{\mathcal{G}} \in \mathbb{G}} P(\widehat{\mathcal{G}} \mid \mathcal{D}) \approx \arg \max_{\widehat{\mathcal{G}} \in \mathbb{G}} \frac{1}{|\mathcal{G}|} \sum_{\mathcal{G}} \sum_{\mathbf{e}_{XY}} \mathbb{1}_{\widehat{\mathcal{G}}}[\mathbf{e}_{XY} \mid \mathcal{D}]. \quad (5)$$

A hyperparameter  $\alpha \in (0, 1)$  is used as a threshold for the values in  $\mathbf{C}$  to prevent irrelevant edges from being included into  $\widehat{\mathcal{G}}$ . Scutari and Nagarajan (2013) and Liao et al. (2022) provide two data-driven choices for its value. Once the threshold is applied, the construction of  $\widehat{\mathcal{G}}$  is performed *greedily*: edges are sorted by decreasing confidence and incrementally added to  $\widehat{\mathcal{G}}$ , skipping those inducing cycles (Algorithm 2). Adapting TMA for cyclic models (Nodelman, 2007; Bregoli et al., 2020; Villa-Blanco et al., 2023) is straightforward.

---

**Algorithm 2:** Threshold-based Model Averaging (TMA).

---

**Input:** A set of DAGs  $\mathcal{G}$  and a threshold  $\alpha \in (0, 1)$ .

**Output:** An average DAG  $\widehat{\mathcal{G}}$ .

```

1 Function TMA( $\mathcal{G}, \alpha$ )
2   /* Phase I - Estimate confidence matrix. */
3    $\mathbf{C} \leftarrow \mathbf{0}$                                 Initialize distribution parameters.
4   for  $\mathcal{G} \in \mathcal{G}$  do                      Iterate over DAGs.
5      $\mathbf{C}[X, Y] \leftarrow \mathbf{C}[X, Y] + \mathbb{1}_{\mathcal{G}}[X, Y], \quad \forall (\mathbf{e}_{XY}) \in \mathbf{E}_{\mathcal{G}}$       Increment counts.
6    $\mathbf{C} \leftarrow \mathbf{C} / |\mathcal{G}|$                       Normalize w.r.t.  $|\mathcal{G}|$ .
7
8   /* Phase II - Threshold and sort by decreasing confidence. */
9    $\tilde{\mathbf{C}} \leftarrow \{(X, Y) \mid \mathbf{C}[X, Y] > \alpha\}$       Set of  $(X, Y)$  tuples s.t.  $\mathbf{C}[X, Y] > \alpha$ .
10   $\tilde{\mathbf{C}} \leftarrow \arg \text{sort } \tilde{\mathbf{C}}$           Sort  $(X, Y)$  tuples in  $\tilde{\mathbf{C}}$  by decreasing  $\mathbf{C}[X, Y]$ .
11
12  /* Phase III - Estimate average DAG. */
13   $\widehat{\mathcal{G}} \leftarrow (\mathbf{V}, \emptyset)$           Initialize an empty DAG.
14  for  $(X, Y) \in \tilde{\mathbf{C}}$  do          Iterate over candidate edges.
15     $\mathcal{G}' \leftarrow (\mathbf{V}, \mathbf{E}_{\widehat{\mathcal{G}}} \cup \{\mathbf{e}_{XY}\})$       Compute new DAG.
16    if  $DAG(\mathcal{G}')$  then          Check if the new DAG is valid.
17       $\widehat{\mathcal{G}} \leftarrow \mathcal{G}'$           Update current DAG.
18
19 return  $\widehat{\mathcal{G}}$ 

```

---

### 3. Model Averaging on Higher-Order Interactions

In this section, we propose a new averaging framework that leverages *higher-order structures* to improve the TMA algorithm. We first introduce the *cover of a graph*.

**Definition 4 (Cover of a Graph)** *Let  $\mathcal{G} = (\mathbf{V}, \mathbf{E})$  be a graph and  $\mathcal{C} = \{\mathbf{E}_{\varphi} : \varphi \in \Phi\}$  be an indexed family of subsets  $\mathbf{E}_{\varphi} \subset \mathbf{E}$  s.t.  $\bigcup_{\varphi} \mathbf{E}_{\varphi} = \mathbf{E}$ , then  $\mathcal{C}$  is said to be a cover of  $\mathcal{G}$ .*

Each index  $\varphi$  corresponds to one and only one set  $\mathbf{E}_{\varphi}$ , so we can use  $\varphi$  for simplicity. In this context,  $\Phi$  is an *index set* for a given graph  $\Phi : \mathbb{G} \rightarrow \{\varphi\}$ . While this definition  $\varphi$  is flexible for identifying subsets of edges, it does not allow to select the edges incident to a given vertex. We introduce the notion of *incident cover* for this purpose.

**Definition 5 (Incident Cover of a Graph)** Let  $\mathcal{G} = (\mathbf{V}, \mathbf{E})$  be a graph and  $\mathcal{C} = \{\mathbf{E}_{\varphi_X} : \varphi_X \in \Phi, X \in \mathbf{V}\}$  be an indexed family of subsets  $\mathbf{E}_{\varphi_X} \subset \mathbf{E}$  s.t.  $\bigcup_{\varphi_X}^{\Phi} \mathbf{E}_{\varphi_X} = \mathbf{E}$  and every edge in  $\mathbf{E}_{\varphi_X}$  is incident on  $X$ , then  $\mathcal{C}$  is said to be an incident cover of  $\mathcal{G}$ .

Note that we only require  $\varphi_X$  to induce a subset  $\mathbf{E}_{\varphi_X}$  of *all* the edges incident to  $X$ , which allows us to define  $\Phi$  flexibly while retaining the *locality* of each  $\varphi_X$ . Moreover, such a definition identifies one and only one  $\varphi_X$  for each vertex  $X \in \mathbf{V}$  for a given  $\mathcal{G}$ . We refer to the index  $\varphi_X$  as the *higher-order structure* of  $X$  and, in turn, to the index set  $\Phi_{\mathcal{G}}$  as the set of the higher-order structures of  $\mathcal{G}$ .

**Example 1 (Parents-based Incident Cover)**

Let the incident cover  $\mathcal{C}$  be indexed by  $\Phi = \{(X, \Pi_X) \mid X \in \mathbf{V}\}$ . Each index is defined as  $\varphi_X = (X, \Pi_X)$  and each subset is  $\mathbf{E}_{\varphi_X} = \{\mathbf{e}_{ZX} \mid Z \in \Pi_X\}$ . In other words, each set  $\mathbf{E}_{\varphi_X}$  in the cover  $\mathcal{C}$  contains all and only the edges induced by the vertex  $X$  and its parents  $\Pi_X$ . The key intuition is that  $\varphi_X$  identifies the relevant variables that interact with  $X$ , rather than just a single variable  $Z$  as in the case of  $\mathbf{e}_{ZX}$ . Figure 1 depicts this case for  $\mathbf{e}_{BC}$  and  $\mathbf{e}_{HI}$ .

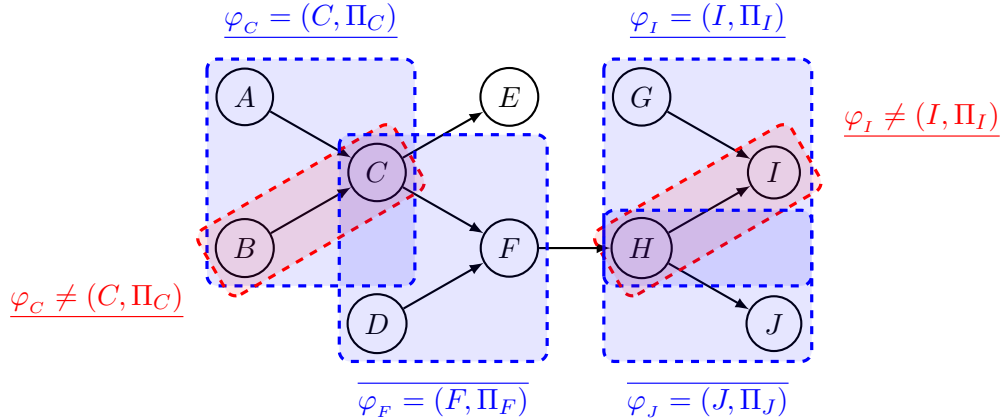


Figure 1: Higher-order interactions are highlighted in blue, compared to lower-order ones in red. Note that  $\varphi_J$  is a special case where higher- and lower-order interactions coincide.

The causal discovery problem is formulated as an optimization problem with an objective function depending on  $P(\mathcal{G} \mid \mathcal{D})$ . We now redefine such an objective function following  $\Phi_{\mathcal{G}}$ :

$$\mathcal{G}^* = \arg \max_{\mathcal{G} \in \mathbb{G}} P(\mathcal{G} \mid \mathcal{D}) = \arg \max_{\mathcal{G} \in \mathbb{G}} P(\mathbf{E}_{\mathcal{G}} \mid \mathcal{D}) = \arg \max_{\mathcal{G} \in \mathbb{G}} P(\Phi_{\mathcal{G}} \mid \mathcal{D}) \quad (6)$$

As for the TMA algorithm, we rely on the expected value  $\mathbb{E}[\Phi_{\widehat{\mathcal{G}}} \mid \mathcal{D}]$  over the set of bootstrapped DAGs  $\mathcal{G}$  to provide an estimate of  $P(\Phi_{\widehat{\mathcal{G}}} \mid \mathcal{D})$ , following the bagging approach.

**Definition 6 (Causal Discovery by Higher-Order Interactions)** Let  $\mathcal{G}^*$  be the true but unknown DAG,  $\mathbb{G}$  the space of DAGs and  $\mathcal{D}$  the data set induced by  $\mathcal{G}^*$ . The causal discovery problem on higher-order interactions consists in solving:

$$\mathcal{G}^* = \arg \max_{\mathcal{G} \in \mathbb{G}} \sum_{\varphi_X}^{\Phi_{\mathcal{G}}} P(\varphi_X \mid \mathcal{D}) \quad (7)$$

where the summation  $\sum_{\varphi_X}^{\Phi_{\mathcal{G}}}$  aggregates higher-order structures  $\varphi_X$  across  $\Phi_{\mathcal{G}}$ .

We leverage [Definition 5](#) to explain [Equation \(7\)](#), providing an estimate of the global posterior  $P(\Phi_{\hat{\mathcal{G}}} \mid \mathcal{D})$  in terms of each local posterior  $P(\varphi_x \mid \mathcal{D})$ . We start by approximating the posterior with an expectation over the distribution of the higher-order structures:

$$\arg \max_{\hat{\mathcal{G}} \in \mathbb{G}} P(\Phi_{\hat{\mathcal{G}}} \mid \mathcal{D}) \approx \arg \max_{\hat{\mathcal{G}} \in \mathbb{G}} \mathbb{E}[\Phi_{\hat{\mathcal{G}}} \mid \mathcal{D}]. \quad (8)$$

This step is an adaptation of [Equation \(3\)](#) in the context of the higher-order structures  $\Phi_{\hat{\mathcal{G}}}$ . We estimate  $\mathbb{E}[\Phi_{\hat{\mathcal{G}}} \mid \mathcal{D}]$  by counting the occurrences of each  $\varphi_x$  across  $\mathcal{G}$ :

$$\arg \max_{\hat{\mathcal{G}} \in \mathbb{G}} \mathbb{E}[\Phi_{\hat{\mathcal{G}}} \mid \mathcal{D}] = \arg \max_{\hat{\mathcal{G}} \in \mathbb{G}} \frac{1}{|\mathcal{G}|} \sum_{\mathcal{G}}^{\mathcal{G}} \sum_{\varphi_x}^{\Phi_{\mathcal{G}}} \mathbb{1}_{\hat{\mathcal{G}}}[\varphi_x \mid \mathcal{D}] \quad (9)$$

Finally, we rearrange the normalization term  $1/|\mathcal{G}|$  and the outer summation  $\sum_{\mathcal{G}}^{\mathcal{G}}$  inside the inner summation  $\sum_{\varphi_x}^{\Phi_{\mathcal{G}}}$  to obtain the local posterior  $P(\varphi_x \mid \mathcal{D})$  for each  $\varphi_x \in \Phi_{\mathcal{G}}$ :

$$\arg \max_{\mathcal{G} \in \mathbb{G}} \frac{1}{|\mathcal{G}|} \sum_{\mathcal{G}}^{\mathcal{G}} \sum_{\varphi_x}^{\Phi_{\mathcal{G}}} \mathbb{1}_{\hat{\mathcal{G}}}[\varphi_x \mid \mathcal{D}] = \arg \max_{\hat{\mathcal{G}} \in \mathbb{G}} \sum_{\varphi_x}^{\Phi_{\mathcal{G}}} P(\varphi_x \mid \mathcal{D}) \quad (10)$$

From [Definition 6](#) and [Equation \(10\)](#), we derive the *Generalized Model Averaging* (GMA) algorithm. Pseudocode is given in [Algorithm 3](#). It is a generic template for causal discovery on higher-order interactions based on  $\mathcal{G}$  and the index set  $\Phi$ :

Phase I - Estimating each  $P(\varphi_x \mid \mathcal{D})$  following [Definition 6](#),

Phase II - Sorting each  $\varphi_x$  depending on the estimated  $P(\varphi_x \mid \mathcal{D})$  terms,

Phase III - Maximizing the posterior probability  $P(\Phi_{\hat{\mathcal{G}}} \mid \mathcal{D})$  greedily s.t.  $\hat{\mathcal{G}}$  is acyclic.

---

**Algorithm 3:** Generalized Model Averaging (GMA).

---

**Input:** A set of DAGs  $\mathcal{G}$ , an index set  $\Phi$  and a threshold  $\alpha \in (0, 1)$ .

**Output:** An average DAG  $\hat{\mathcal{G}}$ .

```

1 Function GMA( $\mathcal{G}, \Phi, \alpha$ )
2   /* Phase I - Estimate posterior distribution. */
3    $\Phi \leftarrow \mathbf{0}$                                 Initialize distribution parameters.
4   for  $\mathcal{G} \in \mathcal{G}$  do                      Iterate over DAGs.
5      $\Phi[\varphi_x] \leftarrow \Phi[\varphi_x] + \mathbb{1}_{\mathcal{G}}[\varphi_x], \quad X \in \mathbf{V}, \varphi_x \in \Phi_{\mathcal{G}}$       Increment counts.
6    $\Phi \leftarrow \Phi / \sum_{\varphi_x} \Phi[\varphi_x]$           Estimate  $P(\varphi_x \mid \mathcal{D})$ .
7
8   /* Phase II - Threshold and sort by decreasing posterior. */
9    $\tilde{\Phi} \leftarrow \{\varphi_x \mid \Phi[\varphi_x] > \alpha\}$       Set of  $\varphi_x$  s.t.  $\Phi[\varphi_x] > \alpha$ .
10   $\tilde{\Phi} \leftarrow \text{arg sort } \tilde{\Phi}$           Sort  $\varphi_x$  in  $\tilde{\Phi}$  by decreasing  $\Phi[\varphi_x]$ .
11
12  /* Phase III - Estimate average DAG. */
13   $\hat{\mathcal{G}} \leftarrow (\mathbf{V}, \emptyset)$           Initialize an empty DAG.
14  for  $\varphi_x \in \tilde{\Phi}$  do          Iterate over higher-order structures.
15     $\mathcal{G}' \leftarrow (\mathbf{V}, \mathbf{E}_{\hat{\mathcal{G}}} \cup \mathbf{E}_{\varphi_x})$       Compute new DAG.
16    if DAG( $\mathcal{G}'$ ) then          Check if new DAG is valid.
17       $\hat{\mathcal{G}} \leftarrow \mathcal{G}'$           Update current DAG.
18
19 return  $\hat{\mathcal{G}}$ 

```

---

The time and space complexity of GMA are as follows. Let  $k = |\mathcal{G}|$ ,  $n = |\mathbf{V}|$  and  $m = |\mathbf{E}|$ :

- The space complexity of  $\mathcal{G}$  is  $\mathcal{O}(kn^2)$ . The worst-case scenario corresponds to the case where the DAGs are dense. However, causal discovery algorithms usually assume that the true DAG is sparse, in which case the space complexity is  $\Theta(km)$  where  $m$  is the average number of edges over  $\mathcal{G}$ .
- The space complexity of the  $\Phi$  is  $\mathcal{O}(kn)$ . In general, the complexity of  $\Phi$  is  $\mathcal{O}(n \cdot 2^n)$  since  $\varphi_X$  takes values in the power set  $2^{\mathbf{V}}$ . However, we store values only for the observed  $\varphi_X$ . Hence, the worst case is where we observe exactly  $k$  distinct  $\varphi_X$  for each vertex  $X$ . Therefore, the final space complexity is  $\mathcal{O}(kn)$ . Furthermore, we are guaranteed that  $\Phi$  is sparse since  $k \ll 2^n$  when the time complexity of obtaining  $\mathcal{G}$  is super-exponential, which is the case for most real-world applications.

In summary, the worst-case space complexity of [Algorithm 3](#) is  $\mathcal{O}(kn^2)$ .

Assuming  $\Phi$  is a sparse matrix with  $\mathcal{O}(n)$  access time, the time complexities for the most relevant lines are as follows:

- Line 3-4, the **for** cycle requires  $\mathcal{O}(kn^2)$  to accumulate the counts.
- Line 5, the element-wise sparse multiplication takes  $\mathcal{O}(kn^2)$ .
- Line 7, sorting  $\widehat{\Phi}$  is equivalent to sort a set with cardinality  $kn$ , hence  $\mathcal{O}(kn \cdot \log(kn))$ .
- Line 8-12, the **for** cycle iterates  $\mathcal{O}(kn)$  times and the inner *DAG* algorithm takes  $\mathcal{O}(n + m)$ , with  $m$  representing the number of edges of  $\widehat{\mathcal{G}}$ . Therefore, the overall time complexity of this block in the worst-case scenario is  $\mathcal{O}(kn \cdot (n + m))$ .

In conclusion, the worst-case time complexity of [Algorithm 3](#) is  $\mathcal{O}(kn \cdot (n + m))$ .

## 4. Experiments

We compared the existing TMA algorithm w.r.t. specific higher-order structures. In particular, we investigated the impact of the choice of higher-order structure by evaluating three GMA variants that differ only in the definition of the index set  $\Phi$ : the set of *parents* (PMA), the set of *children* (CMA) and the set of *incident vertices* (IMA). These methods are evaluated against the DAGs of the reference BN models reported in [Table 1](#), often used as a benchmark for simulation studies. To guarantee complete transparency and reproducibility, experimental results are obtained using open-source software made publicly available [here](#).

### 4.1. Experimental Design

For each reference model  $\mathcal{B}$ , we sample multiple data sets  $\mathcal{D}$  using forward sampling. Each data set has sample size  $|\mathcal{D}| = |\Theta|\rho$ , where  $|\Theta|$  is the number of parameters of  $\mathcal{B}$  and  $\rho$  a sample ratio coefficient in  $[0.1, 0.2, 0.5, 1.0, 2.0, 5.0]$ . For each sample ratio, we generate a training set and a test set for in-sample and out-of-sample validation. Following [Algorithm 1](#), each training set is then resampled to produce a bootstrap set  $\mathcal{G}$  of size 100 using HC and the BIC scoring criterion for causal discovery. Finally, we aggregated the bootstrap set  $\mathcal{G}$

into the average DAG  $\hat{\mathcal{G}}$  following the different model averaging algorithms discussed earlier. The threshold  $\alpha$  is tuned with a grid search and set to 0.5 for TMA and to  $1/(|\mathbf{V}| - 1)$  for PMA, CMA and IMA (Liao et al., 2022).

We computed the following metrics with respect to the true DAG underlying  $\mathcal{B}$ :

- Bayesian Scoring Criterion (BIC): Schwarz (1978) introduced the BIC as an estimate of the complexity of the model. It is part of the *penalized log-likelihood* family, where the penalization term depends on both the number of parameters of the given model and the sample size of the data set from which the model has been learnt:

$$BIC(\Theta | \mathcal{G}, \mathcal{D}) = \log \mathcal{L}(\Theta | \mathcal{G}, \mathcal{D}) - \frac{1}{2} |\Theta| \log |\mathcal{D}|.$$

In the following, `scaled_in_bic` and `scaled_out_bic` are reported as in-sample and out-of-sample estimates of BIC, respectively. To allow for comparison between different sample ratios, a min-max scaler is applied intra-sample ratio. Note that BIC does not require the true causal graph to be given.

- Structural Hamming Distance (SHD): The cardinality of the symmetric difference, denoted as  $\Delta$ , between the edge sets of  $\mathcal{G}$  and  $\mathcal{H}$  (Tsamardinos et al., 2006):

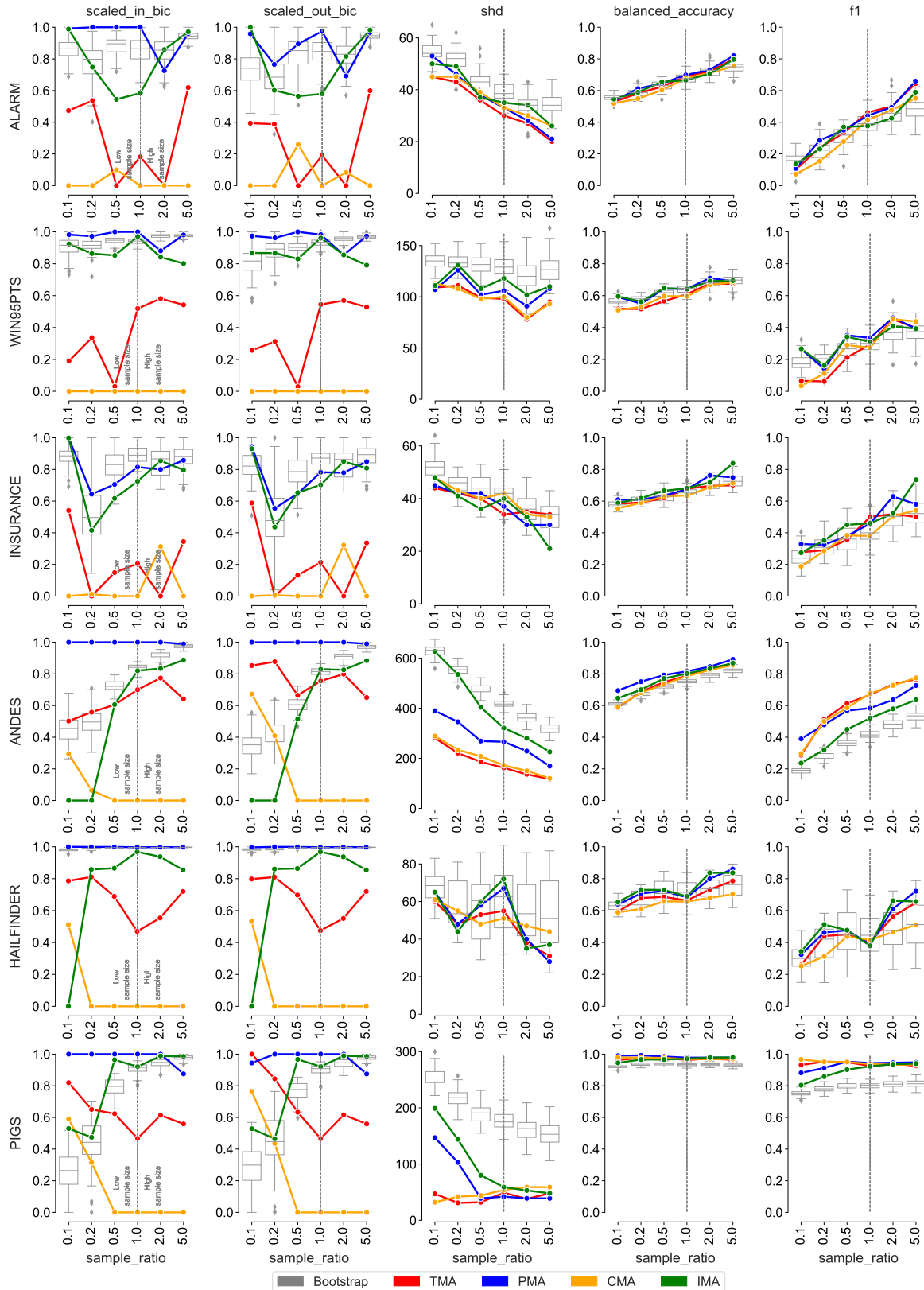
$$SHD(\mathcal{G}, \mathcal{H}) = |\mathbf{E}_{\mathcal{G}} \Delta \mathbf{E}_{\mathcal{H}}| = |(\mathbf{E}_{\mathcal{G}} \setminus \mathbf{E}_{\mathcal{H}}) \cup (\mathbf{E}_{\mathcal{H}} \setminus \mathbf{E}_{\mathcal{G}})|.$$

- Balanced Accuracy & F1 Score: Differences in the adjacency matrices of two graphs can be represented using a *confusion matrix*, especially when  $\mathcal{G}$  is the *predicted* one and  $\mathcal{H}$  is the *true* one, deriving true positives (TP), true negatives (TN), false positives (FP) and false negatives (FN) with the same semantics used in classification problems. To take into account sparsity, we rely on Balanced Accuracy (BA) and the F1 Score:

$$BA = \frac{1}{2} \left( \frac{TP}{TP + FN} + \frac{TN}{TN + FP} \right), \quad F1 = \frac{2TP}{2TP + FP + FN}.$$

Model	Parameters	Vertices	Edges	Avg. M.B.	Avg. Deg.
ALARM	509	37	46	3.51	2.49
WIN95PTS	574	76	112	5.92	2.95
INSURANCE	1008	27	52	5.19	3.85
ANDES	1157	223	338	5.61	3.03
HAILFINDER	2656	56	66	3.54	2.36
PIGS	5618	441	592	3.66	2.68

Table 1: Summary statistics of the DAGs of the reference BNs sorted by increasing number of parameters. Average Markov blanket (Avg. M.B.) and average degree (Avg. Deg.) are computed as the mean of the *Markov blanket* (Koller and Friedman, 2009) and adjacent vertices across each vertex in the vertex set.

Figure 2: Bagging for the reference BNs in [Table 1](#).

## 4.2. Experimental Results

The experimental results are shown in [Figure 2](#). Each subfigure comprises five panels corresponding to the metrics described in the previous subsection. On the horizontal axis, we reported the sample ratio in increasing order; on the vertical axis, we can find the scale of the given metric. SHD takes values in  $[0, +\infty)$ , where the lower, the better; other metrics take values in  $[0, 1]$ , where higher values imply better performance. The proposed algorithms (PMA in blue, CMA in yellow and IMA in green) are compared against the TMA algorithm (in red), which is taken as a baseline. The values of the metrics for the individual bootstrapped DAGs  $\mathcal{G}$  are also shown in grey using box-plots for comparison. The vertical gray-dashed line separates low-sample-size (left) and large-sample-size (right) results.

The PMA algorithm achieves the best in-sample and out-of-sample BIC across every reference DAG, although it is sometimes tied with IMA. This is particularly apparent in low sample size regimes and reference models with many variables. In some cases, for instance, in **ALARM** and **WIN95PTS**, it performs better than any other approach, including the bootstrap set itself. In some cases, we observe higher SHD values for PMA and IMA. Other balanced metrics are in line with the baseline and the bootstrap set, suggesting that the structural differences are inflated by the unbalanced proportion between extra and missing edges. Both TMA and CMA achieve good structural performance but fail to match PMA in terms of score, recovering less-likely DAGs compared to the other alternatives. Finally, IMA recovers acceptable average DAGs in the case of small models and high sample sizes, but its metrics degrade rapidly with the reference model’s complexity.

## 5. Discussion & Conclusions

In this work, we investigated learning an averaged DAG via bagging in the context of causal discovery. In particular, we leveraged higher-order structures to propose a novel theoretical framework, which we used to design a new aggregation algorithm for combining bootstrapped DAGs. We performed a large-scale simulation study on a varied set of reference DAGs to assess the performance of the proposed solution: it dominates state-of-the-art alternatives in structural accuracy and goodness-of-fit, especially under high-dimensional settings and in low-sample size regimes. However, there is still room for improvement. Firstly, considering the topological orderings of the bootstrapped DAGs could mitigate the structural differences in the observed higher-order structures. Secondly, weighting higher-order structures by the scoring criterion could provide additional insights into their goodness of fit. Finally, alternative data-driven thresholds could result in better denoising performance.

## Acknowledgments

Alessio Zanga is funded by F. Hoffmann-La Roche Ltd.

## References

E. Acerbi, T. Zelante, V. Narang, and F. Stella. Gene Network Inference Using Continuous Time Bayesian Networks: A Comparative Study and Application to th17 Cell Differentiation. *Bmc Bioinformatics*, 15(1):387, 2014.

E. Acerbi, E. Viganò, M. Poidinger, A. Mortellaro, T. Zelante, and F. Stella. Continuous Time Bayesian Networks Identify *prdm1* as a Negative Regulator of *th17* Cell Differentiation in Humans. *Scientific Reports* 2016 6:1, 6(1):1–7, 2016.

P. M. Addo, C. Manibialoa, and F. McIsaac. Exploring Nonlinearity on the *co2* Emissions, Economic Production and Energy Use Nexus: A Causal Discovery Approach. *Energy Reports*, 7:6196–6204, 2021.

S. Bongers, P. Forré, J. Peters, and J. M. Mooij. Foundations of Structural Causal Models with Cycles and Latent Variables. *The Annals of Statistics*, 49(5):2885–2915, 2021.

A. Bregoli, M. Scutari, and F. Stella. Constraint-Based Learning for Continuous-Time Bayesian Networks, 2020. URL <https://proceedings.mlr.press/v138/bregoli20a.html>.

D. M. Chickering. Optimal Structure Identification with Greedy Search. *Journal of Machine Learning Research*, 3(3):507–554, 2003.

A. C. Constantinou, Z. Guo, and N. K. Kitson. The Impact of Prior Knowledge on Causal Structure Learning. *Knowledge and Information Systems*, 65(8):3385–3434, 2023.

D. Eaton and K. Murphy. Bayesian Structure Learning Using Dynamic Programming and MCMC. 2007.

N. Friedman and D. Koller. Being Bayesian About Network Structure. A Bayesian Approach to Structure Discovery in Bayesian Networks. 50:95–125, 2003.

N. Friedman, M. Goldszmidt, and A. Wyner. Data Analysis with Bayesian Networks: A Bootstrap Approach. 1999.

C. Glymour, K. Zhang, and P. Spirtes. Review of Causal Discovery Methods Based on Graphical Models. *Frontiers in Genetics*, 10(JUN):524, 2019.

F. Harary and E. Palmer. *Graphical Enumeration*. Elsevier, 1973.

D. Heckerman, D. Geiger, and D. M. Chickering. Learning Bayesian Networks: The Combination of Knowledge and Statistical Data. *Machine Learning*, 20(3):197–243, 1995.

M. Hernán and J. Robins. *Causal Inference: What If?* CRC Press, 2020.

B. Huang, K. Zhang, Y. Lin, B. Schölkopf, and C. Glymour. Generalized Score Functions for Causal Discovery. *Proceedings of the ACM Sigkdd International Conference on Knowledge Discovery and Data Mining*, pages 1551–1560, 2018.

P. Hünermund and E. Bareinboim. Causal Inference and Data Fusion in Econometrics. 2019.

S. Imoto, S. Y. Kim, H. Shimodaira, S. Aburatani, K. Tashiro, S. Kuhara, and S. Miyano. Bootstrap Analysis of Gene Networks Based on Bayesian Networks and Nonparametric Regression. *Genome Informatics*, 13:369–370, 2002.

M. Kocaoglu, A. Jaber, K. Shanmugam, and E. Bareinboim. Characterization and Learning of Causal Graphs with Latent Variables From Soft Interventions. In *Advances in Neural Information Processing Systems*, 2019.

M. Koivisto and K. Sood. Exact Bayesian Structure Discovery in Bayesian Networks. *Journal of Machine Learning Research*, 5:549–573, 2004.

D. Koller and N. Friedman. *Probabilistic Graphical Models: Principles and Techniques*. The MIT Press, 2009.

S. L. Lauritzen. The EM Algorithm for Graphical Association Models with Missing Data. *Computational Statistics and Data Analysis*, 19(2), 1995.

Z. A. Liao, J. D. Duan, and P. Van Beek. On Identifying Significant Edges for Structure Learning in Bayesian Networks. Technical report, 2022.

Y. Liu and A. C. Constantinou. Greedy Structure Learning From Data That Contain Systematic Missing Values. *Machine Learning*, 111(10):3867–3896, 2022.

D. Malinsky and D. Danks. Causal Discovery Algorithms: A Practical Guide. *Philosophy Compass*, 13(1):e12470, 2018.

K. Miley, P. Meyer-Kalos, S. Ma, D. J. Bond, E. Kummerfeld, and S. Vinogradov. Causal Pathways to Social and Occupational Functioning in the First Episode of Schizophrenia: Uncovering Unmet Treatment Needs. *Psychological Medicine*, pages 1–9, 2021.

P. Nandy, A. Hauser, and M. H. Maathuis. High-Dimensional Consistency in Score-Based and Hybrid Structure Learning. *The Annals of Statistics*, 46(6A):3151–3183, 2018.

U. Nodelman. *Continuous Time Bayesian Networks*. PhD thesis, Stanford University, 2007.

J. Pearl. From Bayesian Networks to Causal Networks. In *Mathematical Models for Handling Partial Knowledge in Artificial Intelligence*, pages 157–182. 1995.

J. Pearl, M. Glymour, and N. P. Jewell. *Causal Inference in Statistics: A Primer*. John Wiley \& Sons, 2016.

K. Rantanen, A. Hyttinen, and M. Järvisalo. Discovering Causal Graphs with Cycles and Latent Confounders: An Exact Branch-And-Bound Approach. *International Journal of Approximate Reasoning*, 117:29–49, 2020.

R. Y. Rohekar, Y. Gurwicz, S. Nisimov, G. Koren, and G. Novik. Bayesian Structure Learning by Recursive Bootstrap. 2018.

J. Runge, S. Bathiany, E. Bollt, G. Camps-Valls, D. Coumou, E. Deyle, C. Glymour, M. Kretschmer, M. D. Mahecha, J. Muñoz-Marí, E. H. van Nes, J. Peters, R. Quax, M. Reichstein, M. Scheffer, B. Schölkopf, P. Spirtes, G. Sugihara, J. Sun, K. Zhang, and J. Zscheischler. Inferring Causation From Time Series in Earth System Sciences. *Nature Communications*, 10(1):2553, 2019.

K. Sachs, O. Perez, D. Pe'er, D. A. Lauffenburger, and G. P. Nolan. Causal Protein-Signaling Networks Derived From Multiparameter Single-Cell Data. *Science*, 308(5721):523–529, 2005.

G. Schwarz. Estimating the Dimension of a Model. *The Annals of Statistics*, 6(2):461–464, 1978.

M. Scutari. On the Prior and Posterior Distributions Used in Graphical Modelling. *Bayesian Analysis*, 8(3):1, 2013.

M. Scutari. Bayesian Network Models for Incomplete and Dynamic Data. *Statistica Neerlandica*, 74(3):397–419, 2020.

M. Scutari and R. Nagarajan. Identifying Significant Edges in Graphical Models of Molecular Networks. *Artificial Intelligence in Medicine*, 57(3):207–217, 2013.

M. Singh. Learning Bayesian Networks From Incomplete Data. In *Proceedings of the Fourteenth National Conference on Artificial Intelligence and Ninth Innovative Applications of Artificial Intelligence Conference, AAAI 97, Iaai 97, July 27-31, 1997, Providence, Rhode Island, Usa*, pages 534–539, 1997.

P. Spirtes and K. Zhang. Causal Discovery and Inference: Concepts and Recent Methodological Advances. *Applied Informatics*, 3(1):3, 2016.

P. Spirtes, C. N. Glymour, R. Scheines, and D. Heckerman. *Causation, Prediction, and Search*. MIT Press, 2000.

S. Sugahara, I. Aomi, and M. Ueno. Bayesian Network Model Averaging Classifiers by Subbagging. *Entropy*, 24(5):743, 2022.

S. Triantafillou and I. Tsamardinos. Constraint-Based Causal Discovery From Multiple Interventions Over Overlapping Variable Sets. *Journal of Machine Learning Research*, 16:2147–2205, 2015.

I. Tsamardinos, L. E. Brown, and C. F. Aliferis. The Max-Min Hill-Climbing Bayesian Network Structure Learning Algorithm. *Machine Learning*, 65(1):31–78, 2006.

R. Tu, K. Zhang, P. Ackermann, B. C. Bertilson, C. Glymour, H. Kjellström, and C. Zhang. Causal Discovery in the Presence of Missing Data. 2018.

C. Villa-Blanco, A. Bregoli, C. Bielza, P. Larrañaga, and F. Stella. Constraint-Based and Hybrid Structure Learning of Multidimensional Continuous-Time Bayesian Network Classifiers. *International Journal of Approximate Reasoning*, 159:108945, 2023.

M. J. Vowels, N. C. Camgoz, and R. Bowden. D'ya Like DAGs? A Survey on Structure Learning and Causal Discovery. *ACM Computing Surveys*, 2021.

A. Zanga, A. Bernasconi, P. Lucas, H. Pijnenborg, C. Reijnen, M. Scutari, and F. Stella. Risk Assessment of Lymph Node Metastases in Endometrial Cancer Patients: A Causal Approach. In *Proceedings of the 1st Workshop on Artificial Intelligence for Healthcare (HC@AIxIA)*, 2022a.

A. Zanga, E. Ozkirimli, and F. Stella. A Survey on Causal Discovery: Theory and Practice. *International Journal of Approximate Reasoning*, 151:101–129, 2022b.

A. Zanga, A. Bernasconi, P. J. F. Lucas, H. Pijnenborg, C. Reijnen, M. Scutari, and F. Stella. Causal Discovery with Missing Data in a Multicentric Clinical Study. In *Proceedings of the 21st International Conference of Artificial Intelligence in Medicine (AIME)*, pages 40–44, 2023.